Journal of Catalysis 279 (2011) 381–388

Contents lists available at ScienceDirect

Journal of Catalysis

journal homepage: www.elsevier.com/locate/jcat

Highly durable carbon nanotube-supported Pd catalysts covered with silica layers for the oxygen reduction reaction

Sakae Takenaka [a,*], Noato Susuki [a], Hiroaki Miyamoto [a], Eishi Tanabe [b], Hideki Matsune [a], Masahiro Kishida [a]

[a] *Department of Chemical Engineering, Graduate School of Engineering, Kyushu University, Moto-oka 744, Nishi-ku, Fukuoka 819-0395, Japan*
[b] *Hiroshima Prefectural Technology Research Institute, 3-13-26 Kagamiyama, Higashi-Hiroshima, Hiroshima 739-0046, Japan*

ARTICLE INFO

Article history:
Received 30 December 2010
Revised 16 February 2011
Accepted 19 February 2011
Available online 21 March 2011

Keywords:
Pd catalysts
Silica-coating
Durability of catalysts
Oxygen reduction reaction
Polymer electrolyte fuel cell

ABSTRACT

Pd metal supported on carbon nanotubes (Pd/CNT) for use as a cathode catalyst in polymer electrolyte fuel cells was covered with silica layers a few nanometers thick to improve the durability of the catalyst under severe cathode conditions. The silica-coated Pd/CNT cathode catalyst showed similar activity for the oxygen reduction to Pd/CNT despite coverage of the Pd metal with a silica insulator. In addition, the silica-coated Pd/CNT was highly durable during potential cycling between 0.05 and 1.20 V (*vs.* reversible hydrogen electrode) in aqueous $HClO_4$ while Pd/CNT suffered serious deactivation under the same conditions. The silica layers in the silica-coated Pd/CNT prevent the diffusion of dissolved Pd species from the Pd metal out of the layers. Therefore, silica-coated Pd/CNT was highly durable under the cathode conditions. Furthermore, coverage of Pd/CNT with silica layers inhibited the two-electron reduction of oxygen to H_2O_2.

1. Introduction

Polymer electrolyte fuel cells (PEFCs) are promising devices used for the direct conversion of hydrogen chemical energy into electricity by the oxidation of hydrogen with oxygen [1,2]. Pt metal has been used as a catalytically active metal component for the hydrogen oxidation reaction (HOR) at the anode and for the oxygen reduction reaction (ORR) at the cathode in PEFCs. The sluggish rate of the ORR on Pt compared with the HOR requires more Pt loading in the catalysts at the cathode, which impedes the full commercialization of PEFCs because of the high cost of Pt [3,4]. Recent intensive research efforts toward reducing or replacing Pt catalysts in PEFCs have led to the development of new electrocatalysts for the ORR; these include Pt-based alloys such as Pt–Co and Pt–Pd [5–8]. Pt alloy catalysts show higher activity for ORR than pure Pt metal catalysts. The loading of Pt metal in PEFC cathodes decreases when Pt-based alloy catalysts are used in the cathode. However, the cathode catalysts in the PEFCs are required to work under severe conditions, such as low pH, highly positive potential, high temperature, and an oxygen atmosphere. Under these severe conditions, most catalyst metal species in the cathode inevitably dissolve, which causes a rapid deactivation of the catalysts at the cathode. Because the dissolved metal species diffuse into and deposit on the polymer electrolyte membranes, the dissolution of metal species in cathode catalysts causes a decrease in the conductivity of protons in the polymer electrolyte membranes [9–11]. It is thus desirable to limit the dissolution and diffusion of metals from the catalysts in the cathodes.

The deactivation of Pt catalysts in the cathode impedes the commercialization of PEFCs [12]. Carbon black-supported Pt catalysts that are used in the cathode of state-of-the-art PEFCs should be able to operate under severe conditions such as high potential and low pH. Pt catalysts are deactivated by the aggregation of Pt metal particles on the carbon supports and their activity is decreased as a result of the growth of Pt particles through the dissolution and subsequent deposition of Pt metal (Ostwald ripening) [13–16]. Many research groups have attempted to develop methods to improve the durability of Pt catalysts under severe cathode conditions [12]. The pore structure and functional groups of carbon supports inhibit the aggregation of Pt metal particles to some extent, but these are not effective in suppressing Pt metal dissolution. For the development of Pt or Pt-based alloy catalysts that are highly active and durable during the ORR, it is important to develop methods to suppress the diffusion of metal species out of the catalysts under PEFC cathode conditions.

We previously developed carbon-supported Pt catalysts covered with silica layers a few nanometers thick for use as cathodes in PEFCs [17,18]. The silica-coated Pt catalysts were highly active and had excellent durability for the ORR under PEFC cathode conditions despite the coverage of the Pt metal with a silica insulator. However, Pt catalysts without a silica-coating suffered serious deactivation under the same conditions because of Pt metal particle growth caused by the aggregation of Pt metal particles

---

* Corresponding author. Fax: +81 92 802 2752.
E-mail address: takenaka@chem-eng.kyushu-u.ac.jp (S. Takenaka).

0021-9517/$ - see front matter © 2011 Elsevier Inc. All rights reserved.
doi:10.1016/j.jcat.2011.02.008

and the dissolution and subsequent deposition of Pt metal. The silica layers that are wrapped around the Pt metal prevent the migration of Pt metal particles from the carbon support and prevent the diffusion of dissolved cationic Pt species out of the catalysts. We believe that our silica-coating technique unlocks new ways to develop highly durable non-Pt metal catalysts for the ORR at the cathode in PEFCs, because the coverage of metals with silica layers inhibits the diffusion of metal species out of the catalysts [19].

In this study, Pd metal particles were covered with silica layers. It is well known that Pd metal is highly active during the ORR [20,21]. Pd is a relatively abundant and less expensive resource compared with Pt. However, Pd metal dissolves easily under the cathode conditions in PEFCs. We therefore demonstrate that the coverage of Pd metal particles with silica layers prevents the diffusion of Pd species out of the catalysts. The silica-coated Pd catalysts are highly active and have excellent durability for the ORR under severe cathode conditions.

2. Experimental

2.1. Preparation of catalysts

Multiwalled carbon nanotubes (CNTs) were used as supports for the Pd metal because carbon black, a conventional support for Pt in PEFCs, is easily corroded by oxidation during the accelerated durability test of the catalysts at the cathode by potential cycling [22–25]. CNTs (Wako Pure Chemical Industries) were immersed into a mixed aqueous solution of 8.0 M H_2SO_4 and 8.0 M HNO_3 and then mixed ultrasonically at 328 K for 2 h to oxidize the CNT surfaces [26]. The obtained CNTs were thoroughly washed with distilled water several times and dried in air. The CNTs were dispersed in an aqueous solution containing $PdCl_2$ and dried. The obtained samples were treated in hydrogen at 623 K for 1 h to reduce the Pd precursors to Pd metal. The CNT-supported Pd metal is denoted as Pd/CNT hereafter. The Pd loading in Pd/CNT was determined to be 5.0 wt.% by inductively coupled plasma atomic emission spectroscopy (ICP-AES). The Pd/CNT was covered with silica layers by successive hydrolysis with 3-aminopropyltriethoxysilane (APTES) and tetraethoxysilane (TEOS) [27,28]. The Pd/CNT was dispersed in water and the pH of this solution was adjusted to ca. 10 by the addition of triethylamine. APTES was added to the solution and was then stirred at 333 K for 0.5 h. TEOS was then added to the solution and was stirred at 333 K for 2 h. The obtained samples were dried in air at 353 K and reduced with hydrogen at 623 K for 3 h. The Pd/CNT covered with silica layers is denoted as SiO_2/Pd/CNT hereafter.

2.2. Measurement of cyclic voltammograms

Cyclic voltammograms (CVs) were obtained using a three-compartment electrochemical cell with a Pt mesh and a saturated Ag/AgCl electrode serving as counter and reference electrodes, respectively. The saturated Ag/AgCl electrode was separated from the working electrode compartment by a closed electrolyte bridge. All the potentials are given relative to the reversible hydrogen electrode (RHE). A glassy carbon disk electrode (5 mm diameter) was used as a substrate for the catalysts and polished to a mirror finish. Catalyst ink was prepared by ultrasonically blending 10 mg of the catalyst (Pd/CNT or SiO_2/Pd/CNT) and 5 ml of methanol. A 20-μl aliquot of this ink was deposited on a glassy carbon disk and dried at 333 K. Twenty microliters of a 1 wt.% Nafion solution diluted with methanol was dropped onto the catalysts to ensure that the catalysts attached to the disk. Nafion ionomer (5% Nafion suspension in alcohol, Aldrich) was diluted with methanol to obtain a 1 wt.% Nafion solution before dropping it onto the electrode. The working electrode was immersed in a N_2-purged 0.1 M $HClO_4$ electrolyte solution at 303 K. A solution containing 0.1 M $HClO_4$ electrolyte (Wako Pure Chemical Industries, super special grade) was prepared using deionized water (Millipore, 18 MΩ cm). CVs of the catalysts were measured at a scan rate of 50 mV s^{-1} between 0.05 and 1.20 V. Accelerated durability tests for the catalysts were carried out by cycling the potential of the working electrode in a triangular wave at a scan rate of 50 mV s^{-1} between 0.05 and 1.20 V in N_2-purged 0.1 M $HClO_4$ at 303 K.

2.3. Catalytic evaluation using PEFC single cells

The catalytic activity of Pd/CNT and SiO_2/Pd/CNT for the ORR was examined using PEFC single cells. Cathode catalyst ink for the preparation of the membrane-electrode assembly (MEA) was prepared by ultrasonically mixing Pd/CNT or SiO_2/Pd/CNT with 2-propanol and 5% Nafion ionomer. Anode catalyst ink was prepared by ultrasonically mixing Pt metal (10 wt.%) supported on carbon black (Vulcan XC72, Cabot Co.) with 2-propanol and the Nafion ionomer. The carbon black-supported Pt metal catalysts were prepared by a conventional impregnation method. The average particle diameter of the Pt metal in the catalysts was estimated to be 3.3 nm by the adsorption of CO. We assumed that CO adsorbed onto the surface of the Pt atoms at a mole ratio of CO/Pt = 1. The catalyst ink was painted onto the surface of Teflon-coated carbon paper (5 cm^2, Toray) as a gas diffusion layer. A MEA with an area of 5 cm^2 was fabricated by hot pressing the cathode and anode with Nafion 117 (Aldrich) at 403 K and 10 MPa for 3 min. The MEA was placed on the PEFC single cells (Electrochem. Co., EFC-05-02). Hydrogen (flow rate = 28 ml min^{-1}) and oxygen (flow rate = 28 ml min^{-1}) were supplied to the anode and cathode, respectively. The gases for the cathode and anode were humidified at 353 K before their introduction into the cells. Before obtaining polarization curves for the single cells, MEA was conditioned by the supply of hydrogen to the anode and oxygen to the cathode at a cell voltage of 0.5 V for 1 h. The cell voltage for the single cells was cycled between 0.05 and 1.20 V to perform an accelerated durability test for the catalysts at the cathode. During the durability test, hydrogen and nitrogen were supplied to the anode and cathode, respectively. Polarization curves for the single cells were also measured after the introduction of oxygen to the cathode.

2.4. Catalytic evaluation using a rotating ring-disk electrode

Electrochemical measurements using a rotating ring-disk electrode (RRDE) were carried out using a three-electrode electrochemical cell. A glassy carbon rod (diameter = 6 mm) was used as a counter electrode, and Ag/AgCl was used as a reference electrode. The working electrode was composed of a Pt ring on a 6-mm-diameter glassy carbon core embedded in a Teflon cylinder. Catalyst ink was prepared by ultrasonically blending Pd/CNT or SiO_2/Pd/CNT and methanol. This ink was deposited on a glassy carbon disk. The amount of Pd catalyst deposited onto the glassy carbon rod was such that the Pd content was equivalent in both the experiments. After drying the catalysts at room temperature, the Nafion solution diluted with methanol was dropped onto the catalysts to ensure that the catalysts were attached to the disk. The catalysts were immersed in 0.1 M $HClO_4$ at room temperature. The polarization curves for the ORR on Pd/CNT and SiO_2/Pd/CNT were measured in O_2-saturated 0.1 M $HClO_4$ at room temperature by changing the potential of the working electrode from 0.1 to 1.1 V at a scan rate of 10 mV s^{-1} with an electrode rotation rate of 1600 rpm. The Pt ring electrode was polarized at 1.20 V for the oxidation of hydroperoxide intermediates. Accelerated durability tests for the catalysts were also performed using the RRDE. The potential of the working electrode was cycled between 0.05 and 1.20 V in

N_2-purged 0.1 M $HClO_4$, and then, the polarization curve for the ORR over the catalysts was measured in an O_2-saturated 0.1 M $HClO_4$ electrolyte solution.

2.5. CO stripping experiment

CO stripping voltammograms were measured using a three-compartment electrochemical cell as described for the measurement of the CVs. CO stripping voltammograms for Pd/CNT and SiO_2/Pd/CNT catalysts attached to a glassy carbon rod were measured in a N_2-purged 0.1 M $HClO_4$ solution at 303 K by changing the potential from 0.4 to 1.2 V at a scan rate of 50 mV s^{-1} after the Pd catalysts were immersed in a CO-saturated electrolyte and held at 0.4 V for 30 min. The CO that dissolved into the $HClO_4$ electrolyte was thoroughly purged with pure N_2 for 1 h before obtaining CO striping voltammograms.

2.6. Characterization of the Pd catalysts

Transmission electron microscope (TEM) images of the Pd catalysts were recorded on a JEOL JEM-3000F instrument. Specimens were prepared by ultrasonically suspending the Pd samples in 2-propanol. A drop of the suspension was deposited on a carbon-enhanced copper grid and dried in air.

Structural changes in the Pd species from the Pd/CNT or SiO_2/Pd/CNT cathode catalysts in the MEAs during repeated potential cycling were examined by Pd K-edge extended X-ray absorption fine structure (EXAFS) analysis. The Pd K-edge EXAFS spectra were obtained at the Photon Factory in the Institute of Materials Structure Science, High Energy Accelerator Research Organization, Tsukuba, Japan. Catalyst sample spectra were obtained using a Si(3 1 1) two-crystal monochromator at room temperature with beam line NW10A. The ring energy was 2.5 GeV and the stored current was 250–450 mA (Proposal No. 2010G556). Analysis of the EXAFS data was performed using the EXAFS analysis program REX (Rigaku Co.). A Fourier transformation of the k^3-weighted EXAFS oscillation was performed over a k range from 3.5 to 15.0 Å^{-1}.

3. Results

3.1. Structure of Pd catalysts

Fig. 1 shows TEM images of the Pd/CNT catalysts. Pd metal particles with diameters ranging from 1 to 3 nm were supported on the CNTs, as shown in the TEM images of Pd/CNT. The Pd/CNT catalysts were covered with silica layers by the successive hydrolysis of APTES and TEOS. TEM images of SiO_2/Pd/CNT are also shown in Fig. 1. The SiO_2 loading in SiO_2/Pd/CNT was estimated to be 20 wt.% by ICP-AES. Pd metal particles were also present in the TEM images of the SiO_2/Pd/CNT catalysts, and their particle sizes were similar to that of Pd/CNT. A high-resolution TEM image for SiO_2/Pd/CNT clearly showed the coverage of Pd/CNT with silica layers a few nanometers thick. The SiO_2/Pd/CNT catalysts were calcined at 1073 K in air to confirm whether Pd/CNT was uniformly covered with silica layers. The TEM image of SiO_2/Pd/CNT after calcination in air is shown in Fig. 2. In this TEM image, silica tubes are present, and the inner diameter of the silica tubes is similar to the outer diameter of the CNTs that were used in this study. In addition, Pd metal particles are always present in the silica tube channels, although the size of the Pd metal particles in the silica tubes is significantly larger than the Pd metal particles in SiO_2/Pd/CNT before calcination. The CNTs in SiO_2/Pd/CNT were removed by calcination in air at 1073 K, and silica tubes were formed. Pd metal particles from SiO_2/Pd/CNT should be aggregated in the cavity of the silica tubes during calcination, and the Pd metal particles should grow. The experimental result indicates that the Pd metal particles and

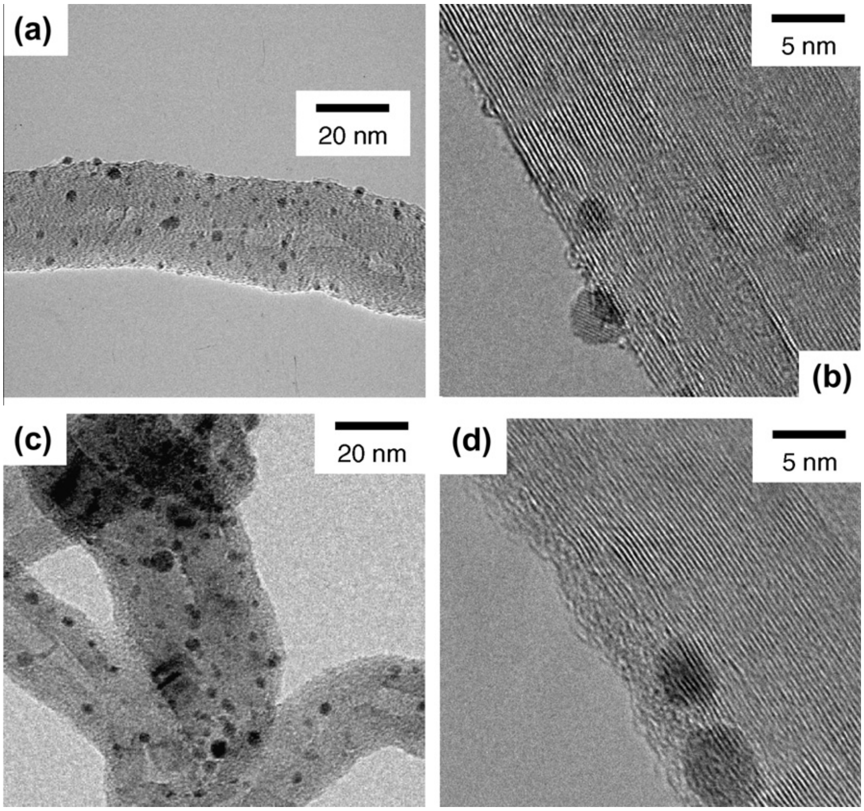

Fig. 1. TEM images of Pd/CNT (a and b) and SiO_2/Pd/CNT (c and d).

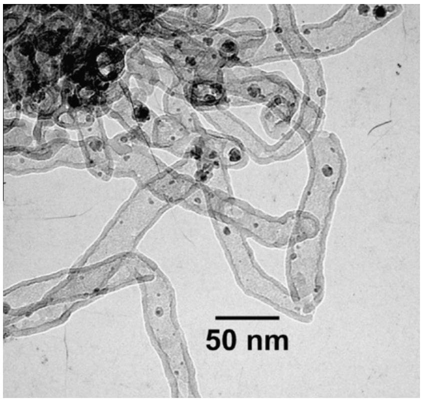

Fig. 2. TEM image of SiO_2/Pd/CNT after calcination in air at 1073 K.

CNTs in SiO_2/Pd/CNT were covered with silica layers a few nanometers thick. In the present study, Pd/CNT was covered with silica layers by the successive hydrolysis of APTES and TEOS. APTES was adsorbed on the CNT surfaces through the interaction between amino groups of APTES and graphene. The APTES adsorbed on the CNT was hydrolyzed to form the thin layers of silica precursors on the CNT. In the subsequent hydrolysis of TEOS on the CNT which was covered with silica precursors from APTES, silica precursors from TEOS should be formed by heterogeneous nucleation and they were uniformly deposited on the CNT, because the silica precursors from APTES work as nucleation sites of silica precursors from TEOS. Therefore, Pd/CNT can be uniformly covered with silica layers by the successive hydrolysis of APTES and TEOS.

3.2. Durability of Pd catalysts

Fig. 3 shows CVs for the Pd/CNT and SiO_2/Pd/CNT catalysts in the N_2-purged $HClO_4$ electrolyte at 303 K. The CVs for these Pd catalysts were also measured in N_2-purged $HClO_4$ after potential cycling between 0.05 and 1.20 V to determine the durability of these Pd catalysts. Two peak couples were present in the CV of the fresh Pd/CNT catalyst. One peak couple at 0.05–0.3 V is attributed to the adsorption and desorption of hydrogen on Pd metal and the other peak couple at 0.5–1.2 V to the oxidation and reduction of Pd metal. The peak currents for the Pd metal in the CVs for Pd/CNT decreased significantly with the number of potential cycles and the peaks disappeared completely after 900 cycles. This is due to the dissolution and diffusion of Pd species in Pd/CNT during potential cycling in the N_2-purged 0.1 M $HClO_4$ electrolyte. On the other hand, two peak couples for the Pd metal were also observed in the CVs of the SiO_2/Pd/CNT catalysts despite the coverage of the Pd metal particles with silica layers. This indicates that the SiO_2/Pd/CNT catalysts are electrochemically active. Reactant molecules such as protons and water diffuse onto the Pd metal surface through porous silica layers during the electrochemical reactions over the SiO_2/Pd/CNT catalysts. We earlier reported that silica-coated Pt metal and silica-coated Pt/CNT show high activity for various catalytic reactions such as the combustion of light alkanes and the hydrogenation of CO [28,29]. The silica layers that are wrapped around the Pt metal particles do not prevent the diffusion of reactants and products. Electrons flow to the Pd metal particles in SiO_2/Pd/CNT through the exposed CNT surfaces. To determine the conduction path of the electrons in SiO_2/Pd/CNT, the electrochemical deposition of Pd metal onto the silica-coated CNT without Pd metal was performed. The silica-coated CNT was attached to a glassy carbon disk electrode and immersed into N_2-purged aqueous HCl containing $PdCl_2$. A TEM image of the silica-coated CNT after the electrochemical deposition of the Pd metal is shown in Fig. 4. The CNTs in the TEM image seem to be covered with silica layers. It should be noted that the Pd metal particles are deposited on the outer surfaces of the silica-coated CNT. The Pd^{2+} cations in the electrolyte solution are reduced to Pd metal on the exposed CNT surfaces during the electrochemical deposition of Pd onto the silica-coated CNT because the exposed CNT surfaces are a conduction pathway for electrons. This result strongly suggests that electrons flow to the Pd metal surface through exposed CNT surfaces during the electrochemical reactions over the SiO_2/Pd/CNT catalysts. SiO_2/Pd/CNT is thus electrochemically active despite the coverage of Pd/CNT with a silica insulator.

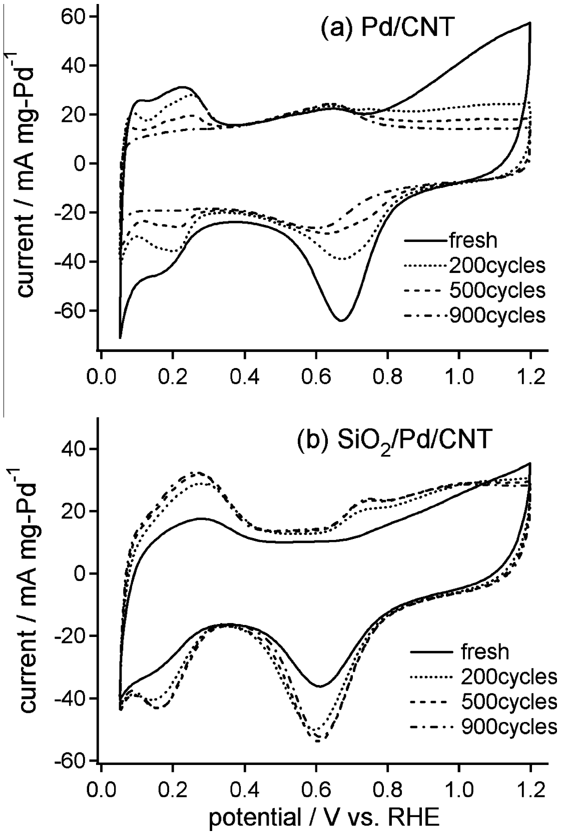

Fig. 3. CVs of Pd/CNT (a) and SiO_2/Pd/CNT (b) in the N_2-purged 0.1 M $HClO_4$ electrolyte during potential cycling between 0.05 and 1.20 V.

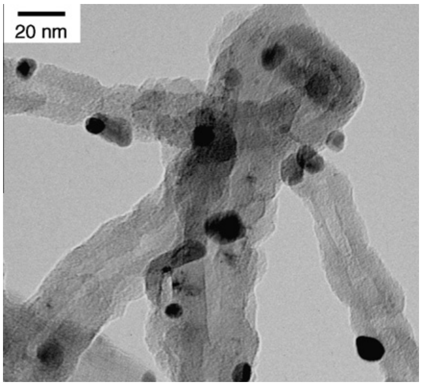

Fig. 4. TEM image of silica-coated CNT after the deposition of Pd metal particles.

Peak currents of the Pd metal in the CVs of SiO_2/Pd/CNT gradually increase up to 500 potential cycles and then remain constant after 500 cycles, while the peak currents in the CV for Pd/CNT reduce significantly with the number of potential cycles. These results indicate that the coverage of Pd/CNT with silica layers improves the durability of the Pd metal during potential cycling in the aqueous $HClO_4$ electrolyte. The silica layers that are wrapped around the Pd metal particles prevent the diffusion of Pd species, which dissolves from the Pd metal, out of the silica layers. Therefore, SiO_2/Pd/CNT shows excellent durability during potential cycling.

Fig. 5 shows TEM images of Pd/CNT and SiO_2/Pd/CNT after 900 potential cycles (shown in Fig. 3). Hardly any Pd metal particles were present in the TEM images of the used Pd/CNT, indicating that the Pd metal particles in the catalyst dissolved during potential cycling in the aqueous $HClO_4$ electrolyte. By contrast, Pd metal particles were present in the TEM images of the used SiO_2/Pd/CNT. Interestingly, the size of the Pd metal particles in the used SiO_2/Pd/CNT was similar to the size of Pd metal particles in the fresh catalyst, and the Pd metal particles in the used catalyst were covered with silica layers as shown in TEM image (d). The Pd metal particles in SiO_2/Pd/CNT also dissolve to form cationic Pd species during potential cycling, because the peak current of the oxidation of Pd metal is present in the CVs of the catalyst. The Pd species that dissolve from the Pd metal in SiO_2/Pd/CNT diffuse out of the silica layers with difficulty and are deposited on the original Pd metal particles. Therefore, the size of the Pd metal particles in SiO_2/Pd/CNT does not change during potential cycling. Furthermore, the Pd metal particles and CNTs in the used SiO_2/Pd/CNT were covered with silica layers a few nanometers thick, suggesting that silica layers in the catalysts were stable under the PEFC cathode conditions.

3.3. Catalytic activity of Pd catalysts for ORR

The catalytic activity of Pd/CNT and SiO_2/Pd/CNT for the ORR was evaluated using RRDE in an O_2-saturated $HClO_4$ electrolyte. The polarization curves for the ORR using these Pd catalysts were also measured after potential cycling between 0.05 and 1.20 V in the N_2-purged $HClO_4$ electrolyte to evaluate the durability of these Pd catalysts. The polarization curves for the ORR on Pd/CNT and SiO_2/Pd/CNT are shown in Fig. 6. The disk current in these polarization curves corresponds to the current of the ORR, while the ring current results from the oxidation of hydroperoxide intermediates on the Pt ring electrode that is polarized at 1.20 V. Fresh Pd/CNT shows catalytic activity for the ORR in the potential region lower than 1.0 V, where the ring current is also higher. Therefore, a two-electron reduction of oxygen to hydroperoxide occurs on the Pd/CNT catalysts in addition to a four-electron reduction to water. The yield of H_2O_2 during the ORR at 0.6 V over fresh Pd/CNT was determined to be 12% assuming a correction efficiency for the ring electrode of 0.38. The catalytic activity of Pd/CNT decreased drastically with the number of potential cycles. This is due to the dissolution and diffusion of Pd metal in the Pd/CNT. By contrast, SiO_2/Pd/CNT showed excellent durability toward potential cycling. The catalytic activity of fresh SiO_2/Pd/CNT is extremely low compared to the activity of fresh Pd/CNT. However, the catalytic activity of SiO_2/Pd/CNT gradually improved with the number of potential cycles, and it remained constant after 1500 cycles. We thus concluded that SiO_2/Pd/CNT had highly durable ORR activity during potential cycling. We compared the catalytic activity of SiO_2/Pd/CNT after 1500 potential cycles to that of fresh Pd/CNT, as shown in Fig. 7. The disk current of the ORR on SiO_2/Pd/CNT after 1500 cycles is slightly lower than that of fresh Pd/CNT, implying that the silica layers that are wrapped around the Pd metal particles work as a diffusion barrier for oxygen and/or protons. The ring current of the SiO_2/Pd/CNT catalysts is considerably lower than that of Pd/CNT. Therefore, the coverage of Pd metal particles with silica layers inhibits a two-electron reduction of oxygen to hydroperoxide. The Pd metal particles in SiO_2/Pd/CNT also form hydroperoxide

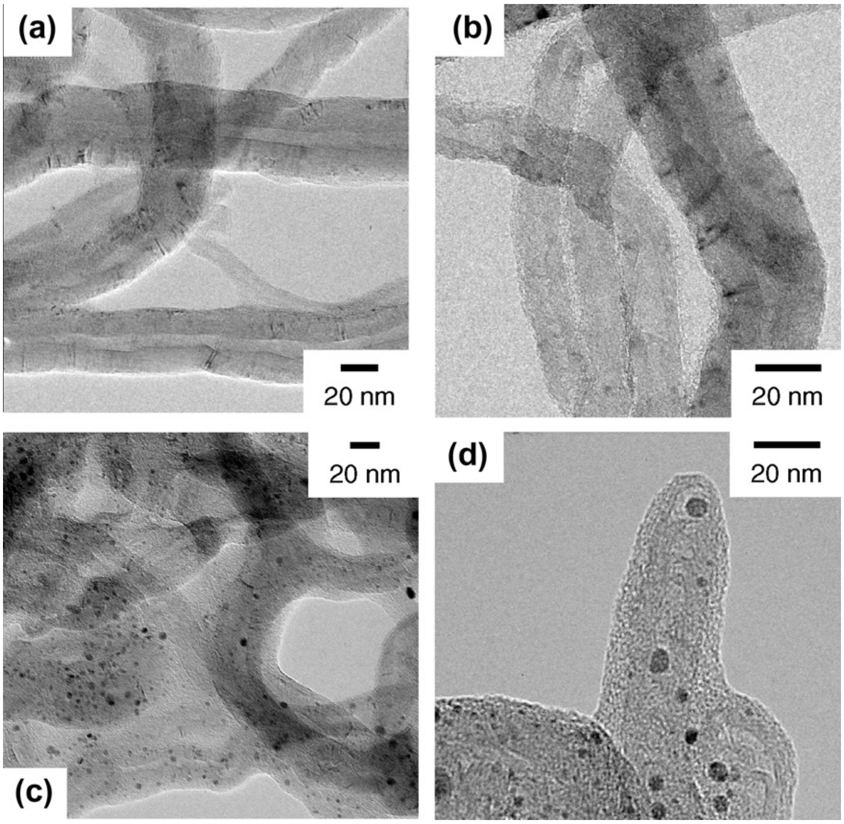

Fig. 5. TEM images of Pd/CNT (a and b) and SiO_2/Pd/CNT (c and d) after 900 potential cycles.

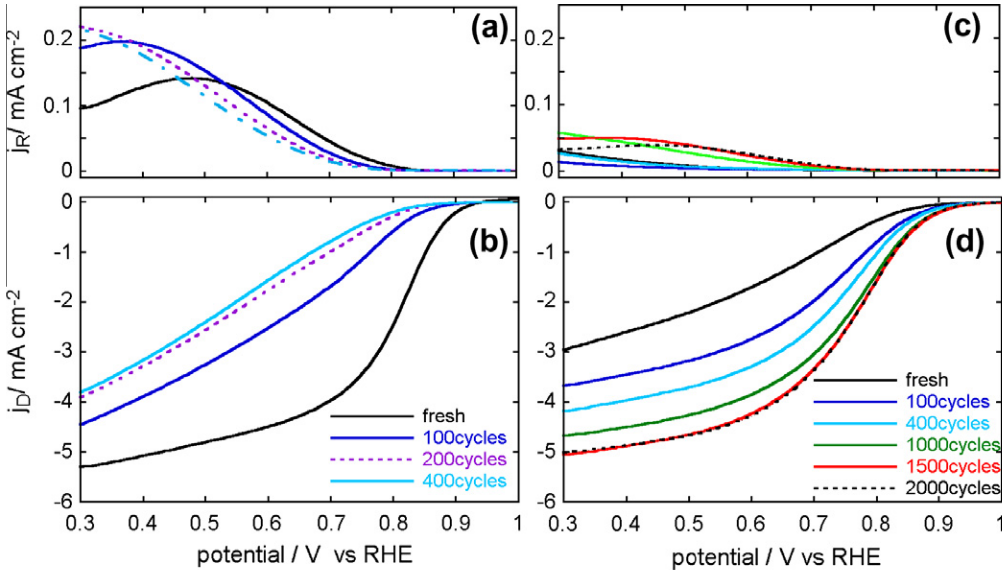

Fig. 6. Polarization curves obtained with a RRDE for the ORR on Pd/CNT (a and b) and on SiO_2/Pd/CNT (c and d) in the O_2-saturated 0.1 M $HClO_4$ electrolyte at room temperature during potential cycling. (a and c) Ring current (current due to the oxidation of hydroperoxide intermediates); (b and d) disk current (ORR current).

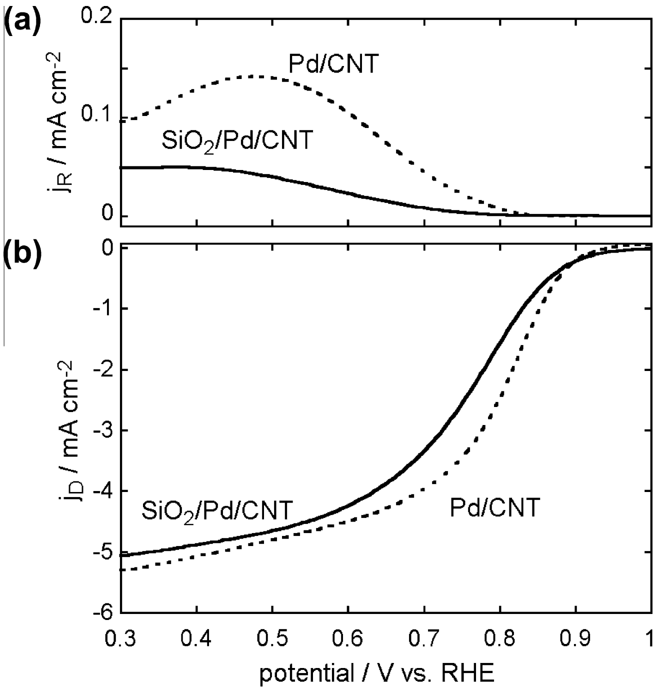

Fig. 7. Polarization curves obtained with a RRDE for the ORR on fresh Pd/CNT and SiO_2/Pd/CNT after 1500 potential cycles in the O_2-saturated 0.1 M $HClO_4$ electrolyte at room temperature. (a) Ring current (current due to the oxidation of hydroperoxide intermediates) and (b) disk current (ORR current).

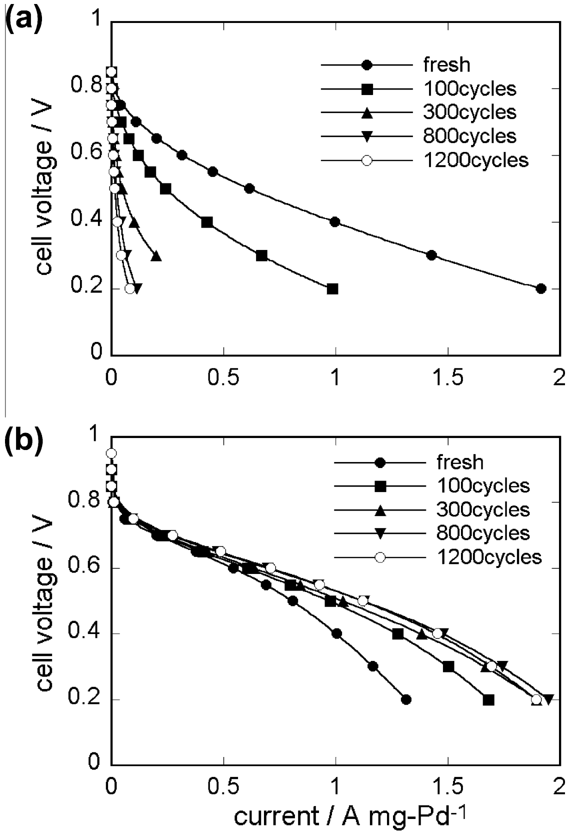

Fig. 8. Polarization curves for PEFC single cells (area of electrode = 5 cm^2) with Pd/CNT (a) or SiO_2/Pd/CNT (b) cathodes during potential cycling. Pd loading in both single cells was 0.1 mg cm^{-2}; cell temperature was 353 K.

during the ORR, but the hydroperoxide diffuses out of silica layers with difficulty. Therefore, the hydroperoxide formed on the Pd metal in SiO_2/Pd/CNT is subsequently reduced to water. The hydroperoxide formed at the cathode in PEFCs oxidizes the carbon support and the polymer electrolyte membranes, which reduces PEFC performance. Therefore, the coverage of Pd/CNT with silica layers is desirable, because of the suppression of hydroperoxide formation from oxygen at the cathode.

The catalytic durability of SiO_2/Pd/CNT during the ORR was also compared with that of Pd/CNT using PEFC single cells. Carbon black-supported Pt catalysts were always used at the anode in the PEFC single cells. The cell voltage of the single cells was repeatedly changed between 0.05 and 1.20 V for the durability test, while nitrogen and hydrogen gases were fed into the cathode and anode in the single cell, respectively. Polarization curves for the PEFC single cells using Pd/CNT or SiO_2/Pd/CNT at the cathode are shown in

Fig. 8. Fresh Pd/CNT showed high activity for the ORR, but the activity of the catalyst decreased rapidly with the number of potential cycles. This is due to the removal of Pd metal from Pd/CNT, as discussed earlier. The catalytic activity of the fresh SiO_2/Pd/CNT catalyst for the ORR was lower than that of the fresh Pd/CNT catalyst. However, the activity of SiO_2/Pd/CNT increased gradually up to 800 potential cycles, and it remained constant after 800 cycles. After 1200 potential cycles, the SiO_2/Pd/CNT showed a similar activity to fresh Pd/CNT. Therefore, the coverage of Pd/CNT with silica layers is effective for the development of cathode catalysts in PEFCs because they are highly active and have excellent durability.

Pd K-edge EXAFS spectra were used to determine structural changes in the Pd species from the Pd/CNT and SiO_2/Pd/CNT cathode catalysts in the PEFC single cells during potential cycling. EXAFS spectra of Pd/CNT and SiO_2/Pd/CNT were obtained just after 300 and 1200 potential cycles, respectively. Fourier transforms of the Pd K-edge k^3-weighted EXAFS spectra (RSFs; radial structure functions) of these Pd catalysts before and after potential cycling are shown in Fig. 9. A strong peak is present at around 2.4 Å in the RSF of fresh Pd/CNT, and the position of this peak is consistent with that of Pd foil. Therefore, the Pd species in fresh Pd/CNT are present as Pd metal. A strong peak at around 2.4 Å was also present in the RSF of Pd/CNT after potential cycling, and its intensity was significantly stronger than that for the RSF of fresh Pd/CNT, indicating the growth of Pd metal crystallites in Pd/CNT during potential cycling [30,31]. As described earlier, Pd metal particles were hardly present on the CNT surfaces in the TEM images of Pd/CNT after potential cycling, as shown in Fig. 5. The Pd metal particles observed in the RSF of the Pd/CNT cathode catalyst in the single cells after potential cycling were present in the polymer electrolyte membrane. It has been reported that the Pt species that dissolves from the Pt cathode catalysts in PEFCs diffuse into polymer electrolyte membranes. The Pt species are reduced by hydrogen that diffused from the anode, and Pt metal particles are deposited in the membrane [16,32]. During potential cycling, Pd metal particles from the Pd/CNT cathode catalysts in the single cell dissolve and diffuse into the polymer electrolyte membrane, where the Pd species are reduced to Pd metal. A strong peak is also present at 2.4 Å in the RSF of fresh SiO_2/Pd/CNT, and the intensity of this peak is very similar to that for the fresh Pd/CNT. Therefore, the crystallite size of the Pd metal in fresh SiO_2/Pd/CNT is the same as that in fresh Pd/CNT. The Pd metal peak, at around 2.4 Å in the RSF of SiO_2/Pd/CNT, did not increase in intensity after potential cycling, indicating that the Pd metal crystallites in the catalysts did not grow during the durability tests. The silica layers that are wrapped around the Pd metal particles prevent the diffusion of the dissolved Pd species out of the silica layers, and the Pd species deposit on the original Pd metal particles. Therefore, the Pd metal particles in SiO_2/Pd/CNT do not grow during potential cycling.

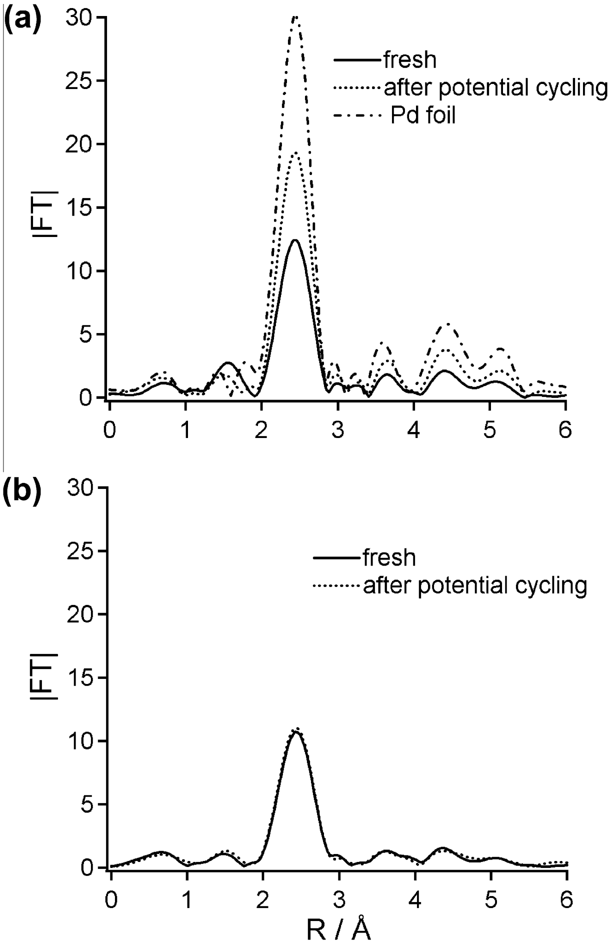

Fig. 9. Fourier transforms of Pd K-edge k^3-weighted EXAFS spectra for Pd/CNT (a) and SiO_2/Pd/CNT cathode catalysts (b) before and after potential cycling.

4. Discussion

The catalytic activity of SiO_2/Pd/CNT for the ORR improved with the number of potential cycles as described earlier. This is due to a rearrangement of the Pd metal surfaces in the catalysts during potential cycling. CO stripping voltammograms for Pd/CNT and SiO_2/Pd/CNT were thus obtained because the peak potentials and the line shapes for CO stripping on the Pd metal surface are characteristic of the type of Pd metal facets [21,33]. Fig. 10 shows

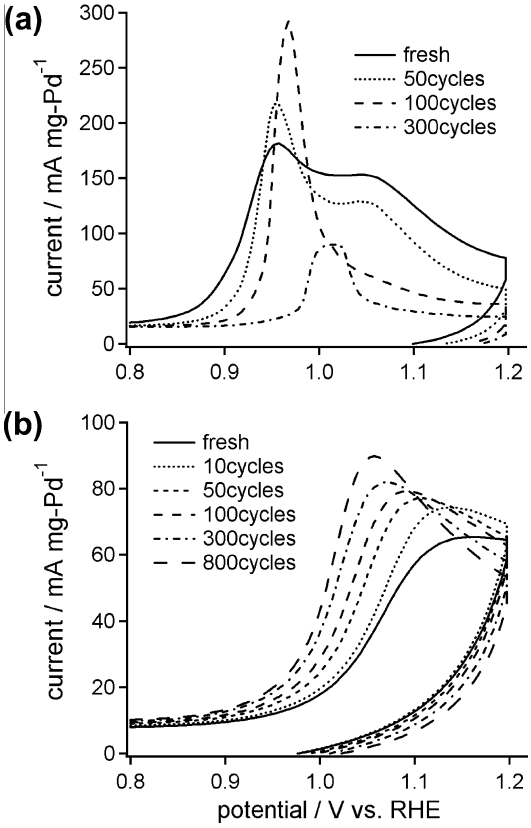

Fig. 10. CO stripping voltammograms for Pd/CNT (a) and SiO_2/Pd/CNT (b) in the 0.1 M $HClO_4$ electrolyte during potential cycling.

CO stripping voltammograms for the Pd/CNT and SiO_2/Pd/CNT catalysts. The CO stripping voltammograms were measured after potential cycling for these Pd catalysts between 0.05 and 1.20 V in the N_2-purged $HClO_4$ electrolyte. CO stripping on fresh Pd/CNT occurred over a broad potential range from 0.85 to 1.1 V. As the number of potential cycles for Pd/CNT increased, the onset potential of the CO stripping gradually shifted to a higher potential and the relative intensity of the peak around 0.95 V increased. However, the peak current for CO stripping over Pd/CNT decreased appreciably after 300 potential cycles. By contrast, the onset potential for CO stripping over SiO_2/Pd/CNT gradually shifted toward a lower potential during potential cycling. CO stripping over fresh SiO_2/Pd/CNT took place in a potential range higher than 1.0 V. The peak onset gradually shifted toward a lower potential, and the peak current increased with the number of potential cycles for SiO_2/Pd/CNT. These results strongly imply that the morphology of the Pd metal in SiO_2/Pd/CNT changed during potential cycling. The catalytic activity of Pd metal for the ORR is sensitive to the type of Pd metal facet [21,34]. Therefore, the catalytic activity of SiO_2/Pd/CNT for the ORR gradually improved during potential cycling. In addition, electrochemically active Pd surface area in SiO_2/Pd/CNT would increase during the potential cycling. As shown in Fig. 3, the peak current due to the adsorption and desorption of hydrogen on Pd metal increased in the CVs for SiO_2/Pd/CNT during the potential cycling. This result suggests that the electrochemically active surface area of Pd metal in SiO_2/Pd/CNT increases during the potential cycling. It is likely that Pd metal particles that are not contacted with CNT surfaces are present in the fresh SiO_2/Pd/CNT. These Pd metal particles in the SiO_2/Pd/CNT are not electrochemically active. However, these Pd metal particles also dissolve under the PEFC cathode conditions such as low pH and oxygen atmosphere. The dissolved Pd species are deposited on CNT surfaces as well as Pd metal particles on the CNT to form Pd metal particles. Thus, the catalytic activity of SiO_2/Pd/CNT is improved during the potential cycling experiments.

Many research groups have attempted to develop non-Pt catalysts for use in PEFC cathodes [35–37]. However, the evaluation of ORR activity for most of the catalysts that contain metal species is difficult, because the metal species inevitably dissolve under PEFC cathode conditions. In this study, we demonstrated that the coverage of non-Pt metals with silica layers a few nanometers thick prevents the diffusion of dissolved metal species out of the catalysts under PEFC cathode conditions. As shown in Fig. 8, the activity of SiO_2/Pd/CNT catalysts for the ORR is inferior to that of Pt catalysts used in state-of-the-art PEFCs. However, the catalytic activity of Pd catalysts for the ORR is improved by the addition of other metal species such as Ti, Co, Mo, and Au [38–40]. The coverage with silica layers should improve the durability of the modified Pd catalysts under the PEFC cathode conditions. Therefore, our silica-coating method is promising for the development of highly active and durable non-Pt catalysts for use in PEFC cathodes.

5. Conclusion

Pd/CNT catalysts for the ORR in PEFCs were covered with silica layers a few nanometers thick to improve the durability of Pd metal under severe PEFC cathode conditions. SiO_2/Pd/CNT showed similar activity for the ORR to Pd/CNT without silica-coating, despite the Pd metal particles being covered with a silica insulator. SiO_2/Pd/CNT showed high durability during potential cycling from 0.05 to 1.20 V. By contrast, Pd/CNT without silica layers greatly deactivated under the same conditions. In addition, the coverage of Pd/CNT with silica layers results in a four-electron reduction of oxygen to water instead of a two-electron reduction of oxygen to hydroperoxide. Therefore, coverage with silica layers is effective for the development of non-Pt cathode catalysts for the ORR in PEFCs.

Acknowledgment

This study was financially supported by the New Energy and Industrial Technology Development Organization (NEDO).

References

[1] G. Brumfiel, Nature 422 (2003) 104.

[2] M.Z. Jacobson, W.G. Colella, D.M. Golden, Science 308 (2005) 1901.

[3] E. Yeager, Electrochim. Acta 29 (1984) 1527.

[4] N.M. Marković, T.J. Schmidt, V. Stamenković, P.N. Ross, Fuel Cells (Weinh.) 1 (2001) 105.

[5] S. Takenaka, A. Hirata, E. Tanabe, H. Matsune, M. Kishida, J. Catal. 274 (2010) 228.

[6] T. Toda, H. Igarashi, H. Uchida, M. Watanabe, J. Electrochem. Soc. 146 (1999) 3750.

[7] V.R. Stamenkovic, B.S. Mum, M. Arenz, K.J.J. Mayrhofer, C.A. Lucas, G. Wang, P.N. Ross, N.M. Markovic, Nature Mater. 6 (2007) 241.

[8] B. Lim, M. Jiang, P.H. Camargo, E.C. Cho, J. Tao, X. Lu, Y. Zhu, Y. Xia, Science 324 (2009) 1302.

[9] T. Okada, Y. Ayata, H. Satou, M. Yuasa, I. Sekine, J. Phys. Chem. B 105 (2001) 6980.

[10] T. Kunimoto, M. Inaba, Y. Nakayama, K. Ogata, R. Umebayashi, A. Tasaka, Y. Iriyama, T. Abe, Z. Ogumi, J. Power Sour. 158 (2006) 1222.

[11] E. Builminot, A. Corcella, F. Charlot, F. Maillard, M. Chatenet, J. Electrochem. Soc. 154 (2007) B96.

[12] R. Borup, J. Meyers, B. Pivovar, Y.S. Kim, Y.R. Mukundan, N. Garland, D. Myers, M. Wilson, F. Garzon, G. Wood, P. Zelenay, K. More, K. Stroh, T. Zawodzinski, J. Boncella, J.E. McGrath, M. Inaba, K. Miyatake, M. Hori, K. Ota, Z. Ogumi, S. Miyata, A. Nishikata, Z. Siroma, Y. Uchimoto, K. Yasuda, K. Kimijima, N. Iwashita, Chem. Rev. 107 (2007) 3904.

[13] G.A. Gruver, R.F. Pascoe, H.R. Kunz, J. Electrochem. Soc. 127 (1980) 1219.

[14] A.C.C. Tseung, S.C. Dhara, Electrochim. Acta 20 (1975) 681.

[15] A. Honji, T. Mori, K. Tamura, Y. Hishimura, J. Electrochem. Soc. 135 (1988) 355.

[16] E. Guilminot, A. Corcella, F. Charlot, F. Maillard, M. Chatenet, J. Electrochem. Soc. 154 (2007) B96.

[17] S. Takenaka, H. Matsumori, K. Nakagawa, H. Matsune, E. Tanabe, M. Kishida, J. Phys. Chem. C 111 (2007) 15133.

[18] S. Takenaka, H. Matsumori, H. Matsune, E. Tanabe, M. Kishida, J. Electrochem. Soc. 155 (2008) B929.

[19] S. Takenaka, N. Susuki, H. Miyamoto, E. Tanabe, H. Matsune, M. Kishida, Chem. Commun. 46 (2010) 8950.

[20] J. Zhang, Y. Mo, M.B. Vukmirovic, R. Klie, K. Sasaki, R.R. Adzic, J. Phys. Chem. B 108 (2004) 10955.

[21] L. Xiao, L. Zhuang, Y. Liu, J. Lu, H.D. Abruña, J. Am. Chem. Soc. 131 (2009) 602.

[22] J. Willsau, J. Heitbaum, J. Electroanal. Chem. 161 (1984) 93.

[23] E. Passalacqua, P.L. Antonucci, M. Vivaldi, A. Patti, V. Antonucci, N. Giordano, K. Kinoshita, Electrochim. Acta 37 (1992) 2725.

[24] K.H. Kangasniemi, K.D.A. Condit, T.D. Jarvi, J. Electrochem. Soc. 151 (2004) E125.

[25] T. Kinumoto, K. Takai, Y. Iriyama, T. Abe, M. Inaba, Z. Ogumi, J. Electrochem. Soc. 153 (2006) A58.

[26] Y. Xing, J. Phys. Chem. B 108 (2004) 19255.

[27] S. Takenaka, T. Arike, H. Matsune, E. Tanabe, M. Kishida, Carbon 46 (2008) 365.

[28] S. Takenaka, T. Arike, H. Matsune, E. Tanabe, M. Kishida, J. Catal. 257 (2008) 345.

[29] S. Takenaka, K. Hori, H. Matsune, M. Kishida, Chem. Lett. 34 (2005) 1594.

[30] K. Teramura, S. Okuoka, S. Yamazoe, K. Kato, T. Shishido, T. Tanaka, J. Phys. Chem. C 112 (2008) 8495.

[31] K. Mori, A. Hanafusa, M. Che, H. Yamashita, J. Phys. Chem. Lett. 1 (2010) 1675.

[32] L. Kim, C.G. Chung, Y.W. Sung, J.S. Chung, J. Power Sour. 183 (2008) 524.

[33] M. Hara, U. Linke, Th. Wandlowski, Electrochim. Acta 52 (2007) 5733.

[34] S. Kondo, M. Nakamura, N. Maki, N. Hoshi, J. Phys. Chem. C 113 (2009) 12625.

[35] Y. Nabae, S. Moriya, K. Matsubayashi, S.M. Lyth, M. Malon, L. Wu, N.M. Islam, Y. Koshigoe, S. Kuroki, M. Kakimoto, S. Miyata, J. Ozaki, Carbon 48 (2010) 2613.

[36] J.L. Fernández, V. Raghuveer, A. Manthiram, A.J. Bard, J. Am. Chem. Soc. 127 (2005) 13100.

[37] K. Sasaki, H. Naohara, Y. Cai, Y.M. Choi, P. Liu, M.B. Vukmirovic, J.X. Wang, R.R. Adzic, Angew. Chem. Int. Ed. 49 (2010) 8602.

[38] O. Savadoga, K. Lee, K. Oishi, S. Mitsushima, N. Kamiya, K. Ota, Electrochem. Commun. 6 (2004) 105.

[39] J.L. Fermández, D.A. Walsh, A.J. Bard, J. Am. Chem. Soc. 127 (2005) 357.

[40] J.L. Fermández, V. Raghuveer, A. Manthiram, A.J. Bard, J. Am. Chem. Soc. 127 (2005) 13100.